Final Master Thesis

Nanofabrication of chemically modified surfaces for large area molecular electronic devices.

Adrián Herrero Lorenzo

Physical Chemistry Department

Supervisors: Santiago Martín Solans and Pilar Cea Mingueza

Academic Year 2021-2022

Title: Nanofabrication of chemically modified surfaces for large area molecular electronic devices.

Author: Adrián Herrero Lorenzo

Supervisors: Santiago Martín Solans and Pilar Cea Mingueza

Physical Chemistry Department

Location: Laboratories of the Platón research group in the Science Faculty, Campus Plaza San Francisco UNIZAR.

Deposition Date: 27/06/2022

ABSTRACT

Current silicon-based technology presents significant drawbacks from a technological and economical point of view. Therefore, molecular electronics is presented as a supporting tool; based on the use of organic or organometallic molecules as basic elements nanoelectronics. This Final Master Thesis aims at the formation of monolayers of a suitably functionalized organic compound, trough the transference of monolayers formed at the air water interface onto solid substrates and how the pH of the subphase can influence on the formation of them, as well as for the study of the surface behaviour of it.

The formation of the monolayers has been carried out using the Langmuir-Blodgett technique and subsequently the films have been characterized both at the air-water interface (Langmuir films) and on the surface of a substrate (Langmuir-Blodgett films) by using a set of techniques such as surface pressure isotherms versus area per molecule, surface potential isotherms versus area per molecule, Brewster angle microscopy (BAM), UV-Vis reflection spectroscopy, atomic force microscopy (AFM), UV-vis absorption spectroscopy, cyclic voltammetry (CV) or quartz crystal microbalance (QCM).

OUTLINE

INTRODUCTION AND BACKGROUND

Electronic devices are present in today's society to such an extent that we cannot imagine life without them right now. These electronic devices have improved their performance exponentially in recent decades due to miniaturization process of the transistors they incorporate, helped by the advances of nanolithography manufacturing techniques mainly.[1]

These continuous improvements are due to the realization of Gordon Moore's idea which can be described using the following sentence: "*Moore's law is the empirical observation that component density and performance of integrated circuits doubles every year*";[2] then revised and corrected to every two years instead of one. This requires reducing the size of the devices in order to increase density. This tendency is reflected in **Figure 1**.

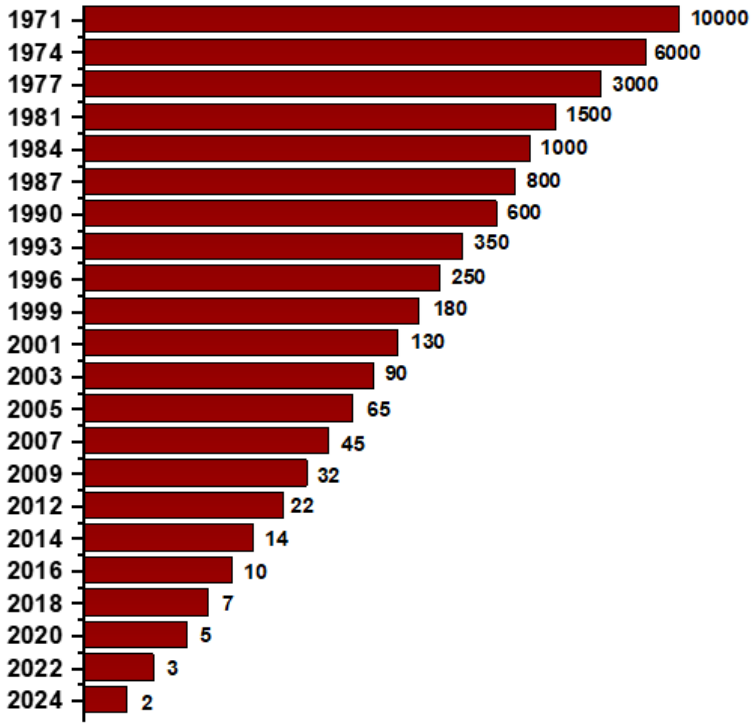

Figure 1. Moore's law tendency to date where the feature size per year in nm can be seen.[3]

At first, semiconductor manufacturers were able to fulfil Moore's law because the size and production price were easily feasible. Over the years, these two features started to decline drastically. This caused several manufacturers to stop producing chips, as it can be observed in **Figure 2**.

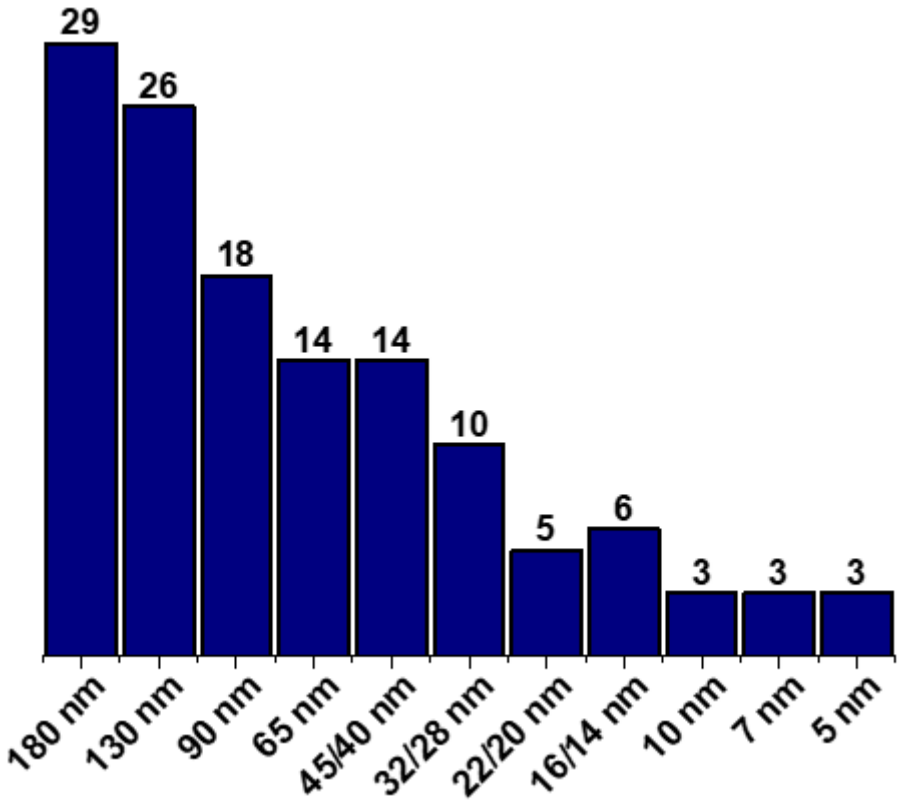

Figure 2. Number of semiconductor manufacturers per chip size.[4]

As **Figure 2** shows, there are only three semiconductor manufacturers that can produce chips these days. They are located in South Korea (Samsung)[5], Taiwan (TSMC)[6] and America (Intel)[7]. It is worthy to mention that Intel has a strong connection with Asia therefore these three manufacturers are mainly Asian. During these past years, there have been also problems related with nanochips and its delivery due to the fact that these important companies are set in Asia.

Other important problem is the elements used to produce these chips. Nowadays, chips are produced using Si, reaching sizes of 5 nm (even smaller in recent studies[8]), but it cannot be used to produce smaller chips due to the loss of its electronic band structure when the material is merely formed by a few silicon atoms. To continue and fulfil Moore's law it is necessary to find an alternative solution to reduce the size of the chips.

Molecular electronics is a clear option in order to solve these problems. It is defined as the technology that uses a molecule or groups of molecules to accomplish the electronic functions of other elements, but with the benefits of the properties of molecules.

Considering this simple definition, it is possible to see that molecular electronics is going to be especially useful in order to fulfil Moore's law because there is a large number of molecules with interesting electronic properties smaller than 5 nm.[9]

OBJECTIVES

The objectives set for this Final Master Thesis can be divided into academic and scientific. Starting first with academic objectives, they are focused on:

- The control and use of different concepts that have been treated and studied during the completion of the degree and master.
- The learning of new notions that will be closely related to the completion of the FMT.
- Acquire other skills that can be useful both in the academic field and outside it. Among them it is worth highlighting:
    - Teamwork.
    - Obtaining a certain autonomy, to reinforce the knowledge acquired during the development of the practices carried out during the master.
    - The analysis of results and their interpretation in a critical and coherent manner.

Turning now to the scientific objectives, these are:

- The feasibility of forming homogeneous monolayers of the compound under study.
- The characterization of the monolayer formed by means of different techniques that demonstrate its structure in order to verify the functionality of the molecule in future applications.
- The study of the influence of pH on the monolayers formation
- The study of the presence of the anthracene group in the formation of intermolecular π-π* interactions, as well as in the formation of 2D aggregates.

EXPERIMENTAL PART.

This section describes the compound under study, as well as the methods and equipment used for its analysis and the materials used.

1. Compound.

The molecule that has been the subject matter of this thesis will be referred as molecule **1** in the following sections and its structure is showed in **Figure 3**. This compound was synthetized by Dr. Ross J. Davidson from University of Durham, United Kingdom.

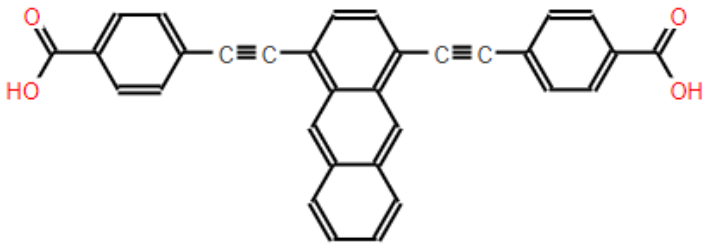

*Figure 3. Structure of compound **1**.*

As it can be seen in **Figure 3**, this molecule presents two hydrophilic carboxylic groups at both ends. These functional groups will act as anchor points to form molecular junctions with metal substrates. This feature is especially useful when studying the molecule using the techniques that will be explain later as this group is influenced by the pH. Additionally, this compound has a hydrocarbon skeleton formed by two phenyl groups linked to an anthracene group trough two alkyne groups. As can be seen, anthracene is not centred with respect to the main axe of the molecule, unlike some similar compounds;[10] which allow us to check how the position of this group can influence on the formation of the monolayer as well as in its electrical properties.

Due to this compound being completely conjugated, monolayers of it are expected to show a good conductivity and, therefore, its possible use as component in molecular electronics. In addition, the anthracene group increases the strength of π-π intermolecular interactions so, the formation of 2D aggregates will be encouraged. These aggregates could also influence in the orientation of the molecules in the monolayer as well as in the electrical properties.

To dissolve this compound, a 4:1 mixture of chloroform:ethanol, respectively was used. Chloroform because this is the "ideal" one to be used in the Langmuir-Blodgett technique and ethanol to increase the solubility of the compound.

2. Reagents and substrates.

Table 1 shows the reagents used in the Final Master Thesis and Table 2 shows the different substrates on which the monolayer has been transferred.

Table 1. Reagents used in this Final Master Thesis.

Compound	CAS number	Supplier and Purity	Use
Chloroform	66-67-3	Sigma-Aldrich, 99%, stabilized with 1% ethanol	Solvent and cleaning
Ethanol	64-17-5	Panreac, absolute, 99.5%	Solvent and cleaning
Acetone	67-64-1	Panreac, QP, 99,5%	Cleaning
Nitrogen	7727-37-9	Linde, 99,999%	Drying

Table 2. Substrates on which the monolayer has been deposited.

Substrate	Supplier	Use	Cleaning method
Gold/Mica	Georg Albert PVD Beschichtungen	AFM characterization	Washed in ethanol and dried with N_2
Gold	Arrandee	CV of the LB films	Washed with acetone, dried with N_2 and burned.
Quartz	Hellma Analytics	Deposition of LB films and UV-vis characterization	Sonicated with $CHCl_3$ and ethanol and dried with N_2
QCM	QCM 25, Stanford research systems.	Determination of surface coverage	Washed with $EtOH/H_2O$ and $CHCl_3$ and dried with N_2

3. Techniques

3.1. Monolayer formation

The procedure used to fabricate the monolayers of the compound under study is the Langmuir-Blodgett (LB) technique.

3.1.1. Langmuir-Blodgett (LB) technique

This method allows to fabricate a monolayer of the compound under study (Langmuir film) at the air-water interface, which can subsequently be transferred onto a solid substrate (Langmuir-Blodgett film).

To carry out this work, the three Langmuir troughs, shown in **Figure 4**, have been used:

- The first one (left) is a NIMA commercial Langmuir trough with dimensions of 100 x 720 mm^2.
- The second (right) is a double Langmuir trough from KSV-NIMA with dimensions of 75 x 782 mm^2.
- The third one (middle) is a homemade Langmuir trough with dimensions of 210 x 460 mm^2.

Theses Langmuir troughs, although they are of different dimensions, have common elements, **Figure 4**:

- A container made of Teflon where the liquid phase was deposited, which in this case was Milli-Q water of 18.2 mΩ·cm resistivity or a NaOH aqueous solution. The solution of the compound of interest was dispersed on this liquid phase.
- Mobile barriers. These are responsible for reducing the area per molecule available in the Langmuir trough. Due to this compression, the molecules approach and interact, giving rise to the formation of the monolayer.
- A sensor that detects and measures surface pressure, Wilhelmy balance.
- A mobile arm (dipper) whose function is to hold the substrate on which the monolayer was transferred.

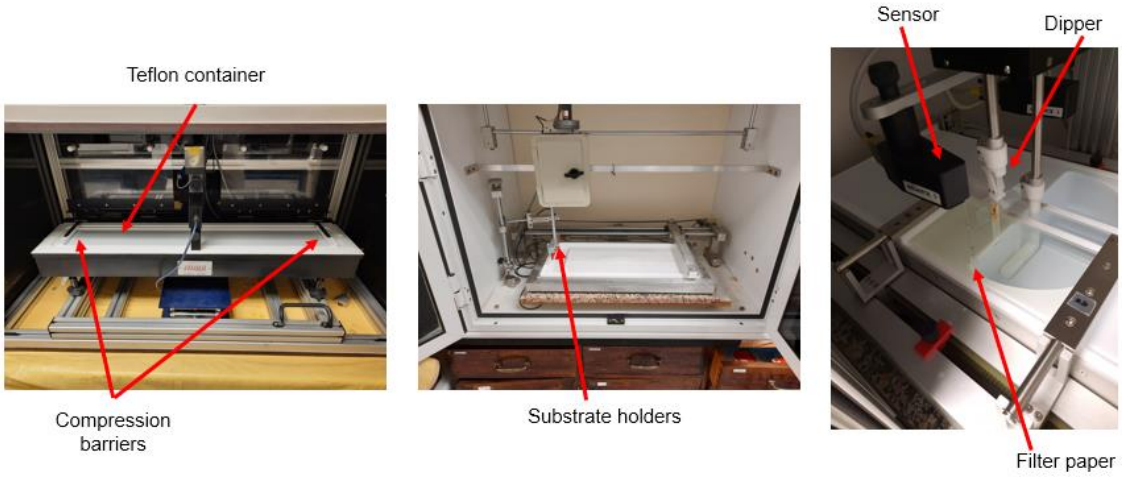

Figure 4. The three types of Langmuir trough used in this Final Master Thesis.

During the development of the FMT, additional techniques were used for the characterization of the manufactured monolayers, but all the procedures have in common the dispersion and formation of the monolayer at the air-water interface, as well as the subsequent transfer to a solid substrate. The choice of substrate depends on the information to be obtained and therefore on the characterization technique to be used to extract said information.

Before starting with the dispersion, the Langmuir trough must be cleaned with acetone and chloroform. When enough time has elapsed for the solvents to evaporate, the cleaning process continues by washing with Milli-Q water, at least 3 times. Once this process has been carried out, the Langmuir trough is considered to be clean and proceeds to fill it with the chosen subphase, Milli-Q water or a NaOH aqueous solution (pH ~ 11), until the formation of an observable meniscus.

The dispersion of the solution of the compound under study (which must be immiscible with the liquid phase) is carried out with a Hamilton-type syringe. It should be done as close to the surface as possible, drop by drop, and a reasonable time (30 minutes) should be allowed for the solvent to evaporate.

At the end of this period, the area per molecule can be reduced by means of the compression movement of the barriers. Once a certain pressure or area per molecule has been reached, the "dipper", which holds the substrate of interest and which has been previously submerged in the subphase, is extracted so that the monolayer formed at the air-water interface can be transferred over it.

3.2. Characterization techniques

The techniques used for the characterization of both the Langmuir and LB monolayers are:

3.2.1. Langmuir monolayers

3.2.1.1. Surface pressure - area per molecule (π-A) isotherms

The surface pressure can be defined as the difference between the surface tension of the water (γ_0) and that of the water in the presence of the film (γ), **equation 1**.

As mentioned, during the formation of the monolayer the area per molecule is reduced by the compressive movement of the barriers. The reduction of the area per molecule causes the surface pressure to increase since there is an increase in the interactions between the molecules that make up the monolayer.

The surface pressure is recorded by a sensor, Wilhelmy sensor. This sensor is connected to a filter paper which in turn is in contact with the subphase because it is partially immersed in it. The filter paper is subjected to a force (ΔF) that in this case will be produced by the difference in surface tension that has been mentioned:

$$\Delta F = 2w(\gamma - \gamma_0) = 2w\pi \qquad \textbf{(1)}$$

where w is the perimeter of the filter paper.

The sensor is connected to a computer that controls the compression process in such a way that the evolution of π is recorded while the area per molecule decreases, that is, the π-A isotherm is registered.

All the isotherms recorded during the completion of the Final Master Thesis have been performed at a compression speed of the barriers of 8 cm^2/minute.

3.2.1.2. Surface potential-area per molecule (ΔV-A) isotherms

This technique provides information on the different phases and phase transitions that can occur during the monolayer formation process.

In this technique, the surface potential is measured using a plug-in module of the KSV-NIMA. In this method, two electrodes are used and placed below (within the subphase) and above (a short distance) from the monolayer, respectively. Once this is

done, the upper electrode vibrates to a determined frequency, generating an alternating current in the capacitor. The molecules that are in the air-water interface have an associated dipole moment, when compressed with the movement of the barriers, their orientation changes and consequently the dipole moment varies, causing the surface potential that is recorded to vary in the ΔV-A isotherms. These isotherms are registered simultaneously to the surface pressure isotherms.

3.2.1.3. Brewster Angle Microscopy (BAM)

This technique is based on the change in the refractive index that occurs at the air-water interface due to the presence of the monolayer.

When a beam of p-polarized light is incident on the air-water interface with an angle of incidence equal to Brewster's angle (53^0 for the water-air interface)[11], no reflection occurs. However, this situation changes when there is a monolayer present at the interface since the refractive index changes and therefore part of that light beam is reflected, reaching a detector where it is analysed. This technique provides "in situ" images of the monolayer formation process, allowing detecting the presence of aggregates or the collapse of the monolayer.

A micro-BAM from KSV-NIMA composed of a red laser of 659 nm wavelength and 50 mW power, and of a CCD camera of 640 x 480 megapixels resolution that possesses a lateral resolution of 12 μm, has been used to obtain images of the monolayer formation process. To obtain images with adequate quality, it will be necessary to incorporate a black glass at the bottom to prevent the microscope used from absorbing the radiation coming from the bottom of the Langmuir trough.

3.2.1.4. UV-Vis reflection spectroscopy

This technique provides information about the presence of two-dimensional aggregates in the monolayer as well as the molecular orientation.

This technique is based on the measurement of the fraction of light reflected at the air-water interface. It is only a fraction since most of the light from the perpendicularly incident beam is transmitted and collected in the light trap. The reflected light will be different depending on the presence or absence of the monolayer.

To record the different spectra, a NanofilmRefSpec2 reflection spectrophotometer was used. The characteristics of this spectrophotometer are the following:

- The working range it presents is from 240 to 1000 nm.
- As a light source, it uses a lamp made up of two (one deuterium and one tungsten) called FiberLight DTM 6/50.

3.2.2. LB films.

3.2.2.1. Atomic Force Microscopy (AFM)

This technique consists of probing the surface of the sample to be analysed with a tip, which is located at the end of a flexible arm (cantilever). This flexible arm bends or flexes depending on the forces (attraction or repulsion) between the tip and the sample surface. A detector measures this bending by the incidence of a laser on the cantilever that is reflected towards a photodiode, obtaining atomic resolution images of the surface. In this way it can be determined whether or not the monolayer has been formed and transferred onto the substrate homogeneously.

The images were obtained with an AFM from Veeco, equipped with a Nanoscope V control unit, operating in "Tapping" mode. The images were taken at a speed of 0.5-1.2 Hz at environmental conditions. RTESPA150 probes from Bruker were used. This AFM belongs to the Singular Scientific and Technical Facility ELECMI (LMA node of the University of Zaragoza).

3.2.2.2. UV-vis absorption spectroscopy

This technique is based on the electronic excitation produced after the absorption of radiation due to the fact that the sample is irradiated with UV-vis radiation. The spectrophotometer used for this task is from Varian, model Cary® 50. All measurements were made with an incidence angle of 90°.

It has been used for the characterization of compound **1** both in solution and in LB monolayer.

3.2.2.3. Cyclic Voltammetry (CV)

Cyclic voltammetry is an electrochemical technique that measures the current generated in an electrochemical cell when a potential variation is applied between the working electrode and the reference electrode. A third electrode that is named counter electrode is also used to control the potential of the working electrodes as a reference in the measurement. In addition, it is also necessary to have in the cell an electrolytic solution, generally a KCl solution.

In this Final Master Thesis, cyclic voltammetry will be used to identify the correct surface pressure to deposit LB films of compound **1** onto a gold substrate, forming the sample in this experiment. In order to achieve this goal, it is necessary to acknowledge that the lower the redox signal in the voltammogram is, the greater is the coverage of the substrate by the molecules.[12]

The samples are not electrochemically active therefore it is necessary to add a redox active specie in order to examine the passivation process on the samples. In this case, a ruthenium complex will be used because it possesses positive charge and possible repulsions with $-COO^-$ groups of **1** will be avoided.

3.2.2.4. Quartz Crystal Microbalance (QCM)

The Quartz crystal microbalance is a highly sensitive technique that allows to determine the mass deposited onto QCM substrates. The operating principle is based on the piezoelectric effect, the reason behind the detection of notably small mass changes, and the material that is used to carry out these measurements is a quartz crystal with gold deposited on both sides. By calculating a change in the oscillation frequency and relating it to the relevant equations, it is possible to determine with nanogram resolution the mass change that has been deposited, which is the final purpose of this technique.[13]

RESULTS AND DISCUSSION

In this section, the results obtained from the experiments carried out and the most relevant conclusions will be presented.

Characterization of compound in solution

First, the characterization of compound **1** in solution was carried out. For this, a series of solutions with different concentrations were prepared and the range of concentrations in which the Lambert-Beer law is followed was verified.

The Lambert-Beer law fits the following linear equation, $A=\varepsilon \cdot l \cdot c$, where A is the absorbance, ε is the molar absorptivity coefficient, l is the thickness of the cuvette (1 mm) and c is the concentration of the solution used. Solutions were prepared using a mixture of chloroform:ethanol (4:1) as solvent and with concentrations ranging between $2.5 \cdot 10^{-5}$ M and $2.5 \cdot 10^{-6}$ M.

As it can be seen in **Figure 5**, the spectra show four main bands:

- Two bands at 270 and 335 nm that can be attributed to the skeleton of the OPE, since at these wavelengths the alkynes and benzenes that can be seen in compound **1** appear
- Two other bands at 420 and 445 nm that are associated with the anthracene group, π-π* transitions that tend to be placed around this wavelength value.

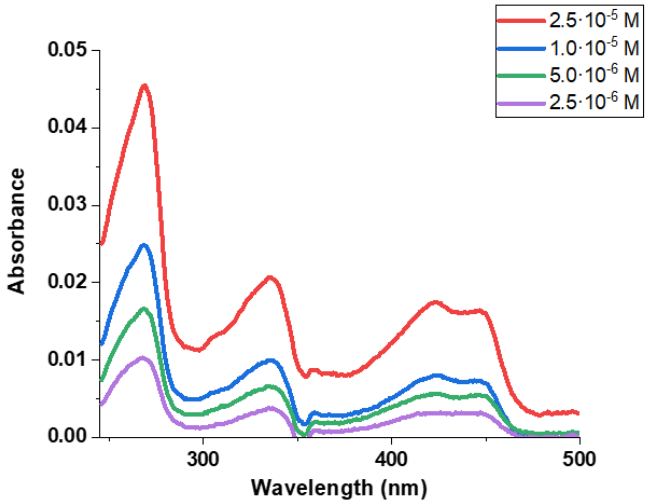

*Figure 5. UV-vis spectra for compound **1** in chloroform:ethanol (4:1) at the indicated concentrations.*

Figure 6 shows a plot of the absorbance versus concentration. In the range of concentrations for which the absorbance measurement has been carried out, the Lambert-Beer law is fulfilled, which allows affirming the absence of three-dimensional aggregates in the solution.

By using the Lambert-Beer law the following molar absorptivities have been obtained: 15030, 7310, 6210 and 5760 $M^{-1} \cdot cm^{-1}$ at 270, 335, 420 and 445 nm, respectively.

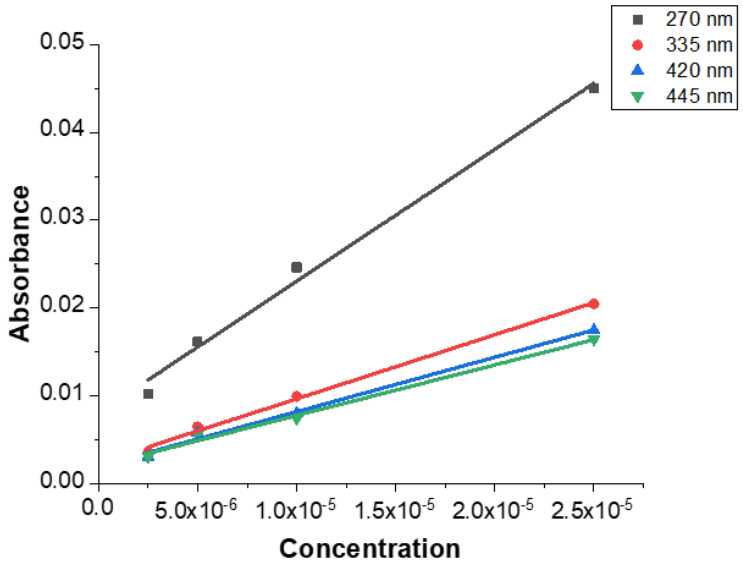

Figure 6. Representation of the Lambert-Beer law for absorption maxima at 270 (black) 335 (red) 420 (blue) and 445 nm (green).

With these results, it was decided to use a solution with a concentration of $1 \cdot 10^{-5}$ M for the conformation of the Langmuir monolayers, since at this concentration the Lambert-Beer law is fulfilled and the formation of three-dimensional aggregates can be ruled out.

Once the behaviour of the compound in solution was determined, a study of the Langmuir monolayers was carried out. During the course of the FMT, two subphases will be used, pure water or a basic pH subphase (pH ~ 11, obtained using a NaOH aqueous solution) for the formation of monolayers with the aim of studying the influence of having the carboxylic acids protonated or not.

Surface pressure vs area per molecule isotherms

Figure 7 shows a representative surface pressure-area isotherm registered using as subphase either pure water or a NaOH aqueous solution (pH 11) at 20 $^{\circ}C$ by dispersing 5 mL of the $1 \cdot 10^{-5}$ M solution of compound **1**. Under these conditions, an area initial of 2.9

nm^2/molecule is obtained when the NIMA commercial Langmuir trough with dimensions of 100 x 720 mm^2 was used. For the other Langmuir troughs, the initial area of 2.9 nm^2/molecule was kept.

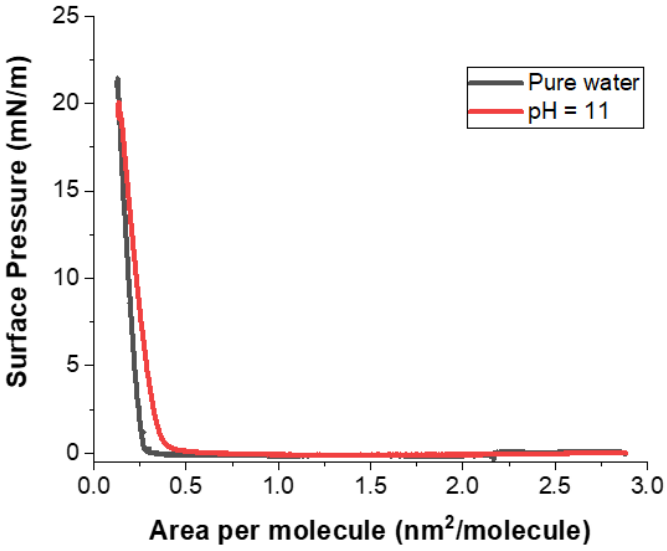

Figure 7. Surface pressure-area per molecule isotherms registered using as subphase either pure water or a NaOH aqueous solution (pH 11) at 20^0C.

According to the isotherm, a classification of the different phases and phase transitions through which the monolayer passes can be made.

At first, the Langmuir film does not change its surface pressure, as it stays close to 0 mN/m, associated to a gas phase in both cases. Then, the surface pressure begins to increase at ca. 0.25 or 0.45 nm^2/molecule for a water subphase or a NaOH aqueous solution, respectively up to 20 mN/m at 0.15 nm^2/molecule. This increase in the surface pressure is associated to a transition to more condensed phase (liquid expanded or even a more condensed phase). At last, the surface pressure decreases confirming the monolayer collapse.

According to **Figure 7**, it is important to highlight the fact that the basic pH isotherm is more expanded. The explanation for this is related to the pH used. Using basic pH, carboxyl groups are deprotonated and become carboxylates. These carboxylates generate greater repulsion and that is why the isotherm is more expanded.

Surface potential vs area per molecule isotherms

Likewise, the ΔV-A isotherms were recorded simultaneously with the π-A isotherms in order to obtain information about the molecular orientation in the monolayer.

Figure 8 shows the normalized surface potential-area per molecule isotherm for both subphases. The normalized surface potential is defined as: the product of the surface potential multiplied by the area per molecule in nm^2.

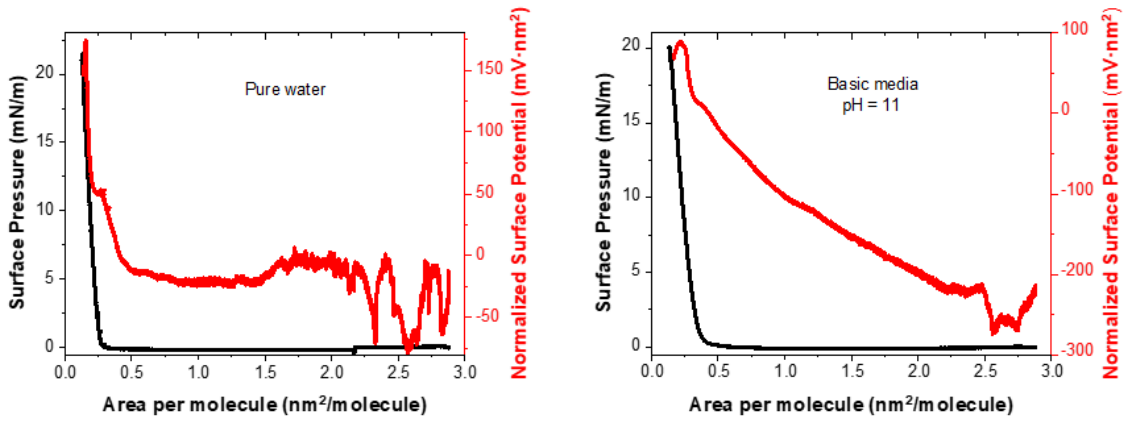

Figure 8. Normalized surface potential – area per molecule isotherms registered using as subphase either pure water or a NaOH aqueous solution (pH 11) at 200C.

As can be seen in **Figure 8**, the two situations represented there can be distinguished:

- Starting with the pure water graphic. From 3.0 to 2.0 nm^2/molecule, oscillations can be seen that can be associated with domains since the monolayer as such has not yet formed. Then, a flat zone with fluctuations can be seen that extends from 2.0 to 0.5 nm^2/molecule. All this region would correspond to the gas phase . From 0.5 nm^2/molecule, the Normalized Surface Potential increases in two different slopes that correspond to a transition from a liquid phase to a more condensed phase (liquid condensed or solid phase. This transition phase could not be seen in the isotherm itself, indicating that this technique is useful for observing more clearly phase transitions. Finally, it can be seen that from 0.15 nm^2/molecule the collapse of the monolayer occurs, related to the decrease in the Normalized Surface Potential.
- With regards to the basic subphase. From 3.0 to 2.5 nm^2/molecule, oscillations in the surface potential are also observed as a consequence of having domains at the air-water interface (high areas per molecule). From here, an increase in slope can

be observed in the Normalized Surface Potential up to 0.25 nm^2/molecule, which can be divided into three zones since at 1.0 nm^2/molecule there is a slight increase in slope as well as at 0.5 nm^2/molecule. This fact can be associated with the fact that up to 1.0 the isotherm is in a liquid expanded phase. From 1.0 to 0.5 nm^2/molecule the isotherm is in a more condensed phase (liquid condensed) and at 0.5 nm2/molecule there is a transition to a solid phase. As in pure water, this phase is not observed in the isotherm itself. Finally, a slope drop can be seen and this is related to the collapse of the monolayer.

Brewster angle microscopy (BAM)

Once the formation of the monolayer at the air-water interface was characterized by recording the surface pressure and surface potential-area isotherms per molecule, Brewster angle microscopy (BAM) was used to obtain "*in situ*" information on the formation process of the monolayer under compression.

Figures 9 and 10 shows different images recorded upon compression. In the images, two clearly differentiated zones can be distinguished: the darkest areas corresponds to zones where there is no monolayer and the greyest and brightest areas are associated to the presence of the monolayer.

In more detail, the images obtained for a pure water subphase show how at 0.80 nm^2/molecule domains of the monolayer are clearly observed and at 0.73 nm^2/molecule practically only organic material is observed, that is, the monolayer is practically formed. At smaller area per molecule values, the images show an increase in brightness associated with an increase in the thickness of the monolayer, that is, the molecules are in a more vertical arrangement in the monolayer.

The situation is a bit different for a basic pH subphase. Here it is possible to see the formation of some aggregates upon the compression process although a monolayer is also formed. Additionally, the brightness of the images is practically the same until 0.32 nm^2/molecule, after that an increase in the brightness is observed as well as the presence of bigger aggregates; revealing the collapse of the monolayer.

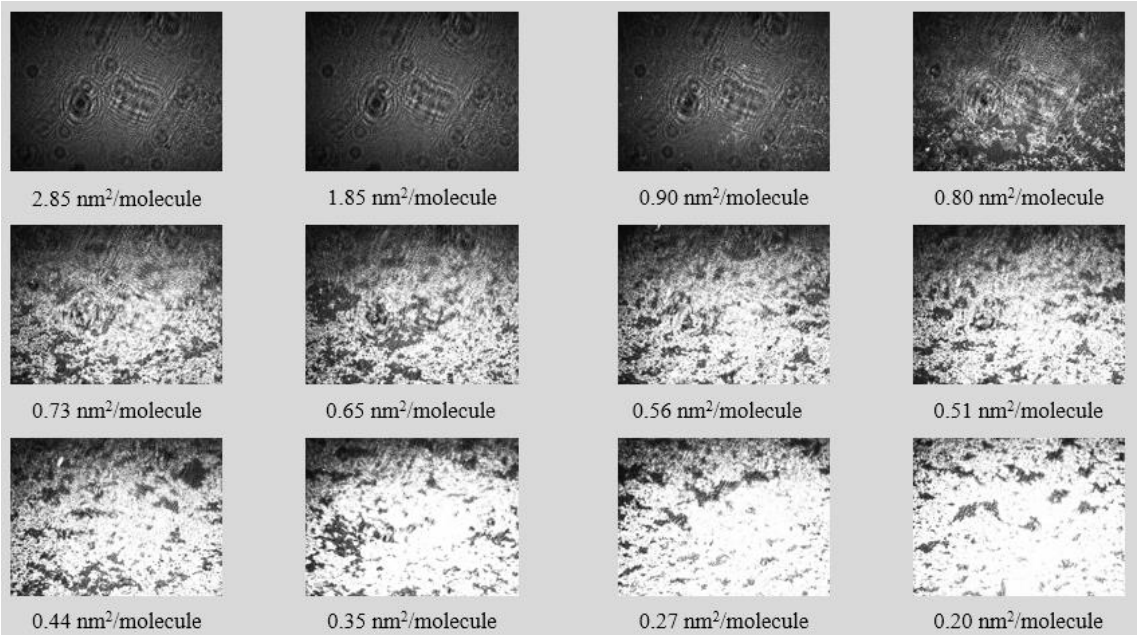

Figure 9. BAM images recorded at the indicated areas per molecule using pure water.

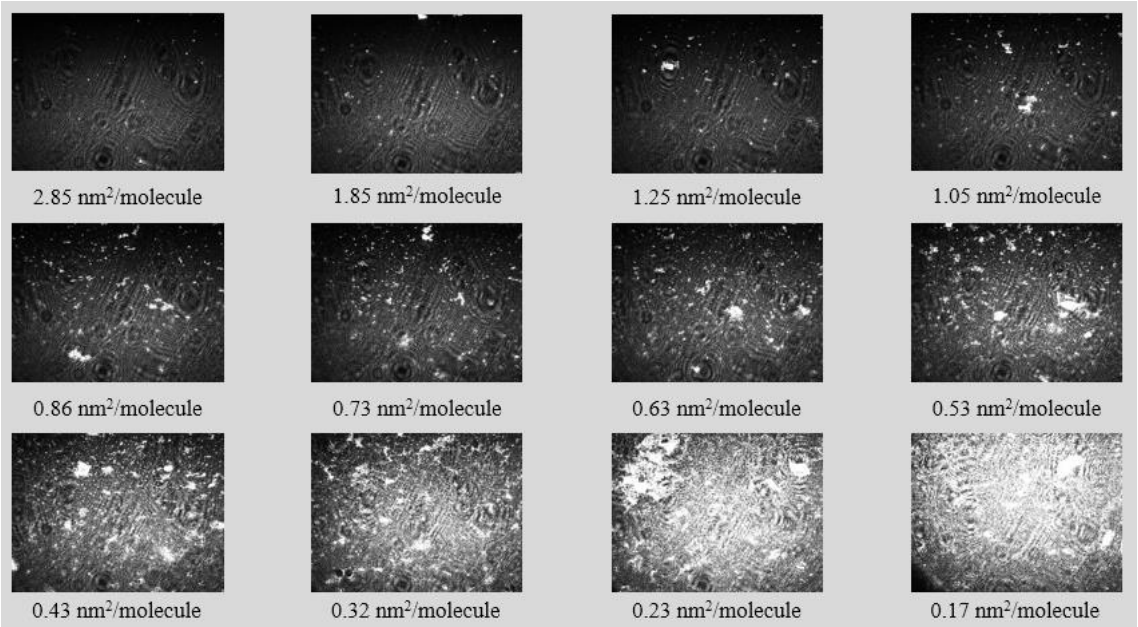

Figure 10. BAM images recorded at the indicated areas per molecule using as subphase a NaOH solution.

Likewise, the images obtained reveal the formation of a monolayer, although this technique is not possible to determine the formation of two-dimensional aggregates. To obtain information on these, UV-vis reflection spectroscopy was used. In addition, this technique can provide information on the orientation of the monolayer during its formation process.

UV-vis Reflection spectroscopy

Figure 11 shows the UV-vis reflection spectra obtained during the compression process when pure water was used as subphase. Under these conditions, three bands are observed mainly:

- A band at 283 nm, which corresponds to the band observed in the UV-vis spectrum of the solution at 270 nm. Therefore, this band shows a shift towards longer wavelengths.
- A band at 353 nm associated to the band observed in the UV-vis spectrum of the solution at 335 nm; which is also shifted towards longer wavelengths.
- At 429 nm that corresponds to the band observed in the UV-vis spectrum in solution at 420 nm. In this case, slightly shift towards longer wavelengths.
- At 485 nm that corresponds to the band observed in the UV-vis spectrum of the solution at 445 nm; in this case the shift is notably higher than in the previous cases.

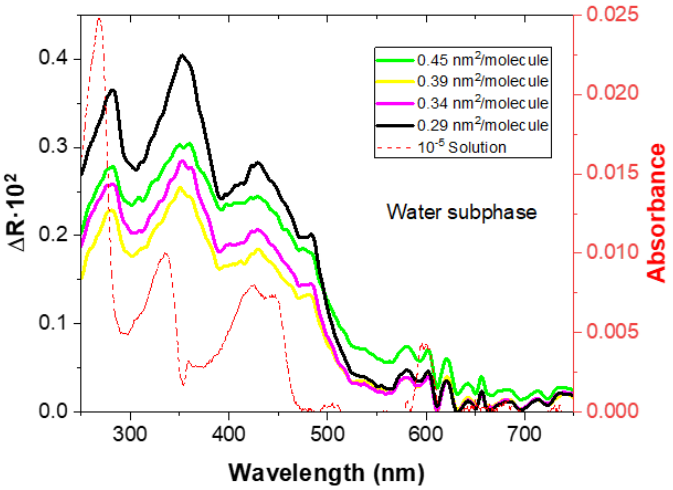

*Figure 11. UV-vis reflection spectra recorded at the indicated areas per molecule and absorption spectrum of a 10^{-5} M solution of **1**.*

Depending on the direction in which the band shifts, we can distinguish between two-dimensional aggregates of type J (bathochromic shift) or two-dimensional aggregates of type H (hypsochromic shift). In this case, the redshift can be attributed to the presence of J-type aggregates[14] in which the angle between the axis of the molecule and the imaginary line through the centre of all the molecules in the monolayer is less than 54^{0}.[15]

As previously mentioned, the anthracene group present in the molecule is related to the increase in molecular interactions and therefore to the formation of this type of aggregates.[16] In the case of the pure water subphase, these aggregates are present, as discussed. On the other hand, in **Figure 12**, it can be seen that the situation at basic pH is quite different from this in pure water.

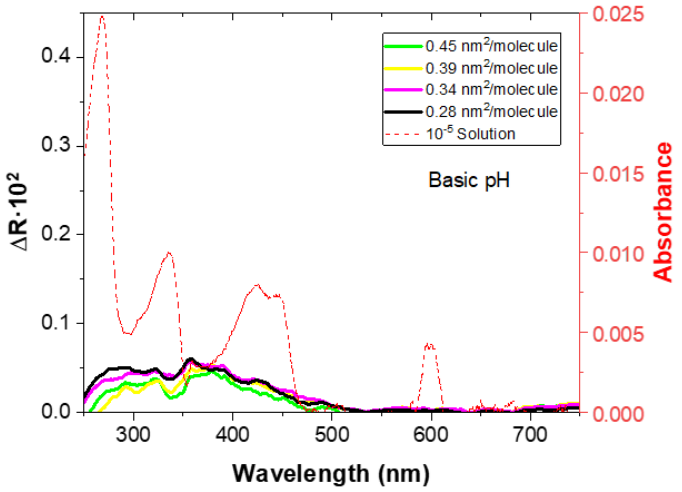

*Figure 12. UV-vis reflection spectra recorded at the indicated areas per molecule when a NaOH subphase was used and absorption spectrum for a 10^{-5} M solution of **1***

As observed in **Figure 12**, the spectra show bands with a very low intensity, even it is difficult to identify the position of them, which probably would be due to the fact that the molecules are almost completely vertical (perpendicular to the surface).

It is observed, overall, for a pure water subphase, that when the area per molecule decreases, the intensity of the bands increases as a consequence of an increase in surface density during the compression process. It is for this reason that the UV-vis reflection spectrum must be normalized in order to eliminate the influence of surface density. To do this, the reflection values have been multiplied by the corresponding area per molecule (in nm^2) at which they were recorded.

$$\Delta R_n = \Delta R \cdot \acute{a}rea$$

Normalized reflection spectra are shown in **Figure 13**.

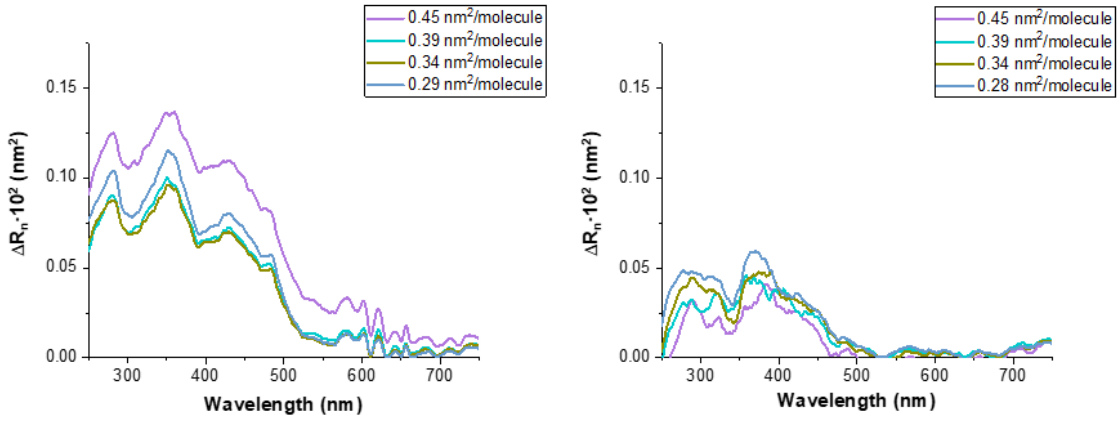

Figure 13. Normalized reflection spectra at the indicated areas per molecule for a pure water subphase (left) for a NaOH solution (right).

As can be seen in **Figure 13**:

- For pure water, the intensity of the bands decreases as the area per molecule decrease. This is attributed to the lifting of the molecules, as observed in the BAM images.
- Whilst, for a basic pH, the molecules stand completely vertical form the beginning of the compression.

Once the formation of the monolayer of compound **1** at the air-water interface (one of the objectives of this FMT) had been demonstrated and characterized as well as the influence of the pH of the subphase studied, the next step was to transfer the monolayer formed at the air-water interface depending on the pH onto a solid support and its characterization.

Atomic force microscopy (AFM)

In order to determine the optimal transfer pressure that allows obtaining homogeneous and compact LB films, transfers were made to different areas per molecule for both subphases. The film that shows the least presence of voids and aggregates will be the optimum transfer pressure. For this, the transferred films were characterized by AFM in order to observe their morphology.

Figure 14 shows the AFM images at the indicated surface pressures when pure water was used as subphase.

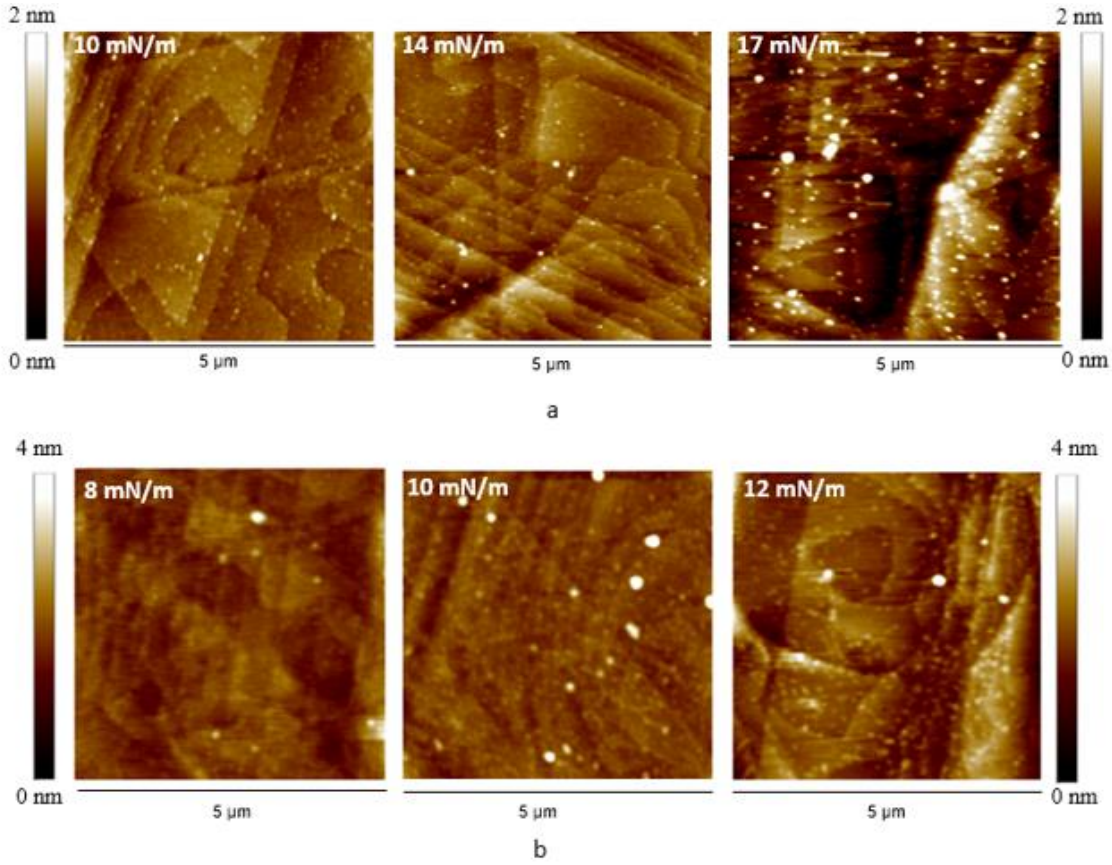

*Figure 14. AFM images for the different LB monolayers of compound **1** transferred onto Au-mica at the indicated pressure; a) Pure water and b) Basic pH.*

From these AFM images we can say that at 10 and 14 mN/m the monolayers are quite homogeneous. Meanwhile, the monolayer at 17 mN/m shows the presence of a great number of aggregates that allow to rule out this pressure to carry out the transference.

Regarding to the basic pH subphase (**Figure 14 b**), the conclusions that can be drawn are quite similar to those of the previous case. The monolayers obtained at 8 and 10 mN/m are quite homogeneous. Meanwhile, the monolayer at 12 mN/m shows the presence of more aggregates and defects.

In addition, through analysis of the AFM images, it is possible to determine the rough mean square (RMS) value. The smaller this value is, the more homogeneous the monolayer is and that will be the chosen transfer pressure. For the aqueous subphase, the RMS values are 0.154, 0.173, and 0.423 nm for 10, 14, and 17 mN/m, respectively. Meanwhile for the basic pH, the RMS values are 0.251, 0.339, and 0.483 for 8, 10, and 12 mN/m, respectively.

Therefore, from the AFM images it can be concluded that the pressures of 17 and 12 mN/m for pure water and basic pH, respectively are not adequate to transfer the monolayers to a substrate. Regarding to the other pressures, RMS values indicate that at 10 and 8 mN/m for pure water and basic pH, respectively, are slightly better than for the other two pressures. To corroborate this information and determine the optimal pressure, the use of the cyclic voltammetry can help us.

Cyclic Voltammetry (CV)

In addition to the AFM images, an indirect evaluation of the morphology of the LB films may be conveniently by means of the cyclic voltammetry (CV)[17]. For that, the electron transfer reaction between a redox couple in an electrolyte solution (0.1 M KCl aqueous solution containing 1 mM $[Ru(NH_3)_6]Cl_3$ as a redox probe)[18] and the underlying gold electrode modified with the different monolayers is studied.

The electrochemical response of the bare gold electrode exhibits a clear voltammetric wave attributed to the redox probe. In contrast, the electrode is largely blocked for the system covered by a LB monolayer of compound **1** transferred at 10 mN/m, indicating a low density of holes in the monolayer. The lower passivation effect for films deposited at low surface pressures indicate that 10 mN/m is an optimum surface pressure of transference. Higher surface pressures of transference did not improve the passivation effect, as it can be seen in **Figure 15.**

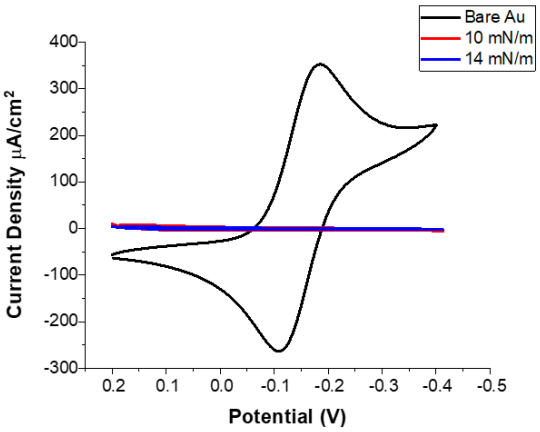

Figure 15. Cyclic voltammograms for a bare gold and LB films transferred to the indicated surfaces pressures using pure water as subphase.

When a NaOH aqueous solution was used, the same factors mentioned before for pure water can be considered.

Therefore, as it can be observed in **Figure 16**, the modified electrodes by a LB film of 1 transferred using the basic subphase is also largely blocked. In this case, when transferring at 8 mN/m, it indicates a low density of holes in the monolayer. This pressure value allows to observe the lowest passivation effect for films deposited indicating that 8 mN/m is an optimum surface pressure of transference. Higher surface pressures of transference did not improve the passivation effect, as it can be seen in **Figure 16**.

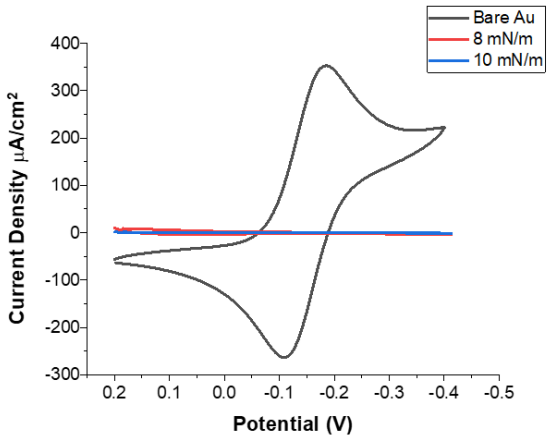

Figure 16. Cyclic voltammograms for a bare gold and LB films transferred to the indicated surfaces pressures using a NaOH aqueous solution..

Summarizing, it can be concluded that the optimum transfer pressures are 10 and 8 mN/m for the aqueous and basic subphase, respectively. These results agree with those obtained by AFM and allow to determine that these are the optimal pressure values for transferring the monolayers.

UV-visible spectroscopy

To elucidate if the structure of the monolayer formed at the air-water interface is maintained during the transference process, UV-visible spectra of the LB film of **1** transferred onto quartz substrates at the optimum transfer surface pressures for both subphases were recorded.

Figure 17 shows the spectrum registered using either water or a NaOH aqueous solution at the optimum surface pressures, at 10 and 8 mN/m, respectively. When a water subphase was used, four bands at 279, 353, 430 and 482 nm are observed. These appears at the same wavelength to these obtained in the reflection spectrum and shifted towards longer wavelengths with respect to the spectrum in solution. That is, the J-aggregates formed at the air-water interface remain during the transfer process.

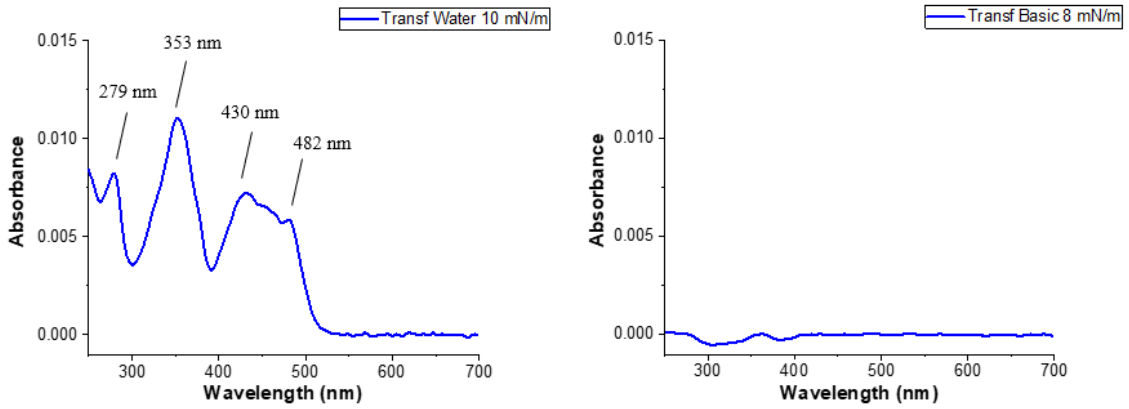

*Figure 17. UV-vis absorption spectrum of a LB film of compound **1**. On the left pure water; on the right basic pH.*

On the contrary, the spectrum registered when a basic subphase was used is clearly different. In this case, clearly differentiated peaks are not observed confirming that the molecules are oriented in a vertical orientation respect to the substrate, as it was observed at the air-water interface.

Quartz Crystal Microbalance (QCM)

Finally, the QCM technique allowed to determine the surface coverage by measuring the variation of a QCM resonator before and after depositing the LB film according to the Sauerbrey equation:[19]

$$\Delta m = -C_F \cdot \Delta f$$

where Δf is the resonance frequency variation, C_f is the sensitivity factor with a value of 56.6 Hz·cm^2/μg and Δm the mass increment.

Considering this equation, the mass deposited at the optimum transfer surface pressure for both subphases was calculated. For pure water, a variation of 10 Hz in the QCM resonator was measured, therefore:

$$\Delta m = \frac{-10}{-56.6 \frac{Hz \cdot cm^2}{\mu g}} = 0.177 \frac{\mu g}{cm^2}$$

or

$$0.177 \frac{\mu g}{cm^2} \cdot \frac{1 g}{10^6 \mu g} \cdot \frac{1}{466.12\ g/mol} = 3.790 \cdot 10^{-10} \frac{mol}{cm^2}$$

Meanwhile for a NaOH subphase:

$$\Delta m = \frac{-11}{-56.6 \frac{Hz \cdot cm^2}{\mu g}} = 0.194 \frac{\mu g}{cm^2}$$

$$0.194 \frac{\mu g}{cm^2} \cdot \frac{1g}{10^6 \mu g} \cdot \frac{1}{466.12\, g/mol} = 4.169 \cdot 10^{-10} \frac{mol}{cm^2}$$

As it can be seen, the change in frequency and by ender in mass are greater when a basic pH is used; which is attributed to have a deposition slightly larger when a basic pH is used as a consequence of having a more vertical arrangement of the molecules.

The determined surface coverage for the LB films can be compared with the are per molecule at the transfer surface pressure:

For a pure water subphase:

- QCM results:

$$\Delta m = 3.790 \cdot 10^{-10} \frac{mol}{cm^2}$$

- Langmuir Film:

At 10 mN/m, the area per molecule is equal to 0.19 nm^2/molecule. Considering this, it is possible to transform this value into mol/cm^2 as follows:

$$0.19 \frac{nm^2}{molecule}; \quad \frac{1}{0.19} = 5.26 \frac{molecules}{nm^2} = 5.26 \cdot 10^{14} \frac{molecules}{cm^2}$$

Now, the Avogadro's number has to be considered to transform the molecules into mol so the comparisons can be done.

$$\frac{5.26 \cdot 10^{14}}{6.022 \cdot 10^{23}} = 8.740 \cdot 10^{-10} \frac{mol}{cm^2}$$

As it can be observed, the surface coverage of a Langmuir monolayer at air-water interface at 10 mN/m is higher than this for a LB film transferred at this pressure; indicative that during the transference process a change in the orientation of the molecules towards a less tilt orientation, as it is observed by UV-vis where the bands are clearly more observable respect to the reflexion spectra.

Meanwhile for a basic subphase:

- QCM results:

$$\Delta m \ = 4.169 \cdot 10^{-10} \frac{mol}{cm^2}$$

- Langmuir Film:

At 8 mN/m, the area per molecule is equal to 0.25 nm^2/molecule. Considering this, it is possible to transform this value to mol/cm^2 following the same steps as before:

$$0.25 \frac{nm^2}{molecule}; \quad \frac{1}{0.25} = 4.00 \frac{molecules}{nm^2} = 4.00 \cdot 10^{14} \frac{molecules}{cm^2}$$

$$\frac{4.00 \cdot 10^{14}}{6.022 \cdot 10^{23}} = 6.642 \cdot 10^{-10} \frac{mol}{cm^2}$$

In this case, both values are more similar revealing that practically the same orientation is keeping under the transference process although with the molecule in less tilt orientation in the LB film, in concordance with the UV-vis respect to the reflexion ones.

CONCLUSIONS AND FUTURE PERSPECTIVES

The experiments carried out allow us to conclude that:

- The compound, which has been denoted as **1**, can form monolayers at the air-water interface using as subphase both pure water as a NaOH aqueous solution. This fact has been verified by means of the surface pressure-area per molecule and surface potential-area isotherms as well as by BAM.
- The optimum transfer surface pressure for fabricating homogenous and free of defects LB films are 10 mN/m and 8mN/m for pure water and basic pH respectively, as evidenced by AFM and more specifically by CV.
- Both the monolayer formed at the air-water interface and the LB film show the formation of two-dimensional J-type aggregates when pure water is used. In the case of basic pH, the molecules are oriented practically in a vertical position respect to the substrate.

In conclusion, it can be stated that the work carried out in this FMT shows that it is feasible to obtain homogeneous and well-packed monolayers of compound **1** using the LB technique, optimizing the manufacturing and transfer conditions on a solid support. Being the future step to be carried out, although it is outside the objectives of this FMT, the measurement of the electrical properties of the LBs and to see the influence of pH as well as the presence of J-type aggregates in their formation.

BIBLIOGRAPHY

1. Lopes AM, Machado JAT, Galhano AM. Empirical laws and foreseeing the future of technological progress. *Entropy*. 2016; 18 (6). doi:10.3390/e18060217

2. Thompson SE, Parthasarathy S. Moore's law: the future of Si microelectronics. *Elsevier*. 2006; 9 (6): 20-25. doi:10.1016/S1369-7021(06)71539-5

3. Hebner K, Priest WW, Chan MW. Moore's Law & the Race for the Rest of the Chessboard. *Epoch*. 2021

4. Technology Node. Accessed January 27, 2022. https://en.wikichip.org/wiki/technology_node

5. Samsung. Accessed January 27, 2022. https://en.wikichip.org/wiki/Samsung

6. TSMC. Accessed January 27, 2022. https://en.wikichip.org/wiki/TSMC

7. Intel. Accessed January 27, 2022. https://en.wikichip.org/wiki/Intel

8. Jeong J, Yoon JS, Lee S, Baek RH. Comprehensive Analysis of Source and Drain Recess Depth Variations on Silicon Nanosheet FETs for Sub 5-nm Node SoC Application. *IEEE Access*. 2020; 8: 35873-35881. doi:10.1109/ACCESS.2020.2975017

9. Carroll RL, Gorman CB. The genesis of molecular electronics. *Angewandte Chemie-International Edition*. 2002; 41 (23): 4379-4400. doi:10.1002/1521-3773(20021202)41:23<4378::AID-ANIE4378>3.0.CO;2-A

10. Lacruz Vaquero; Trabajo Fin de Grado, *Fabricación de Estructuras Bidimensionales Para Dispositivos Electrónicos Moleculares*. Universidad de Zaragoza, 2020.

11. Meunier J. Why a Brewster Angle Microscope? *Colloids and Surfaces A-Physicochemical and Engineering aspects*. 2000; 171 (1-3): 33-40. doi:10.1016/S0927-7757(99)00555-5

12. Cea P, Lopez MC, Martin S, Villares A, Pera G, Giner I. The Use of Cyclic Voltammetry To Probe the Passivation of Electrode Surfaces by Well-Ordered Self-Assembly and Langmuir-Blodgett Films An Advanced Undergraduate Laboratory Experiment in Surface Science and Nanomaterials Chemistry. *Journal of Chemical Education*. 2009; 86 (6): 723-725. doi:10.1021/ed086p723

13. Alassi A, Benammar M, Brett D. Quartz crystal microbalance electronic interfacing systems: A review. *Sensors (Switzerland)*. 2017; 17 (12). doi:10.3390/s17122799

14. Li X, Zhang L, Mu J. Formation of new types of porphyrin H- and J-aggregates. *Colloids and Surfaces A: Physicochemical and Engineering Aspects*. 2007; 311 (1-3): 187-190. doi:10.1016/j.colsurfa.2007.06.015

15. Ballesteros LM, Martín S, Cortés J, et al. Controlling the structural and electrical properties of diacid oligo(phenylene ethynylene) langmuir-blodgett films. *Chemistry - A European Journal*. 2013; 19 (17): 5352-5363. doi:10.1002/chem.201203261

16. Balasaravanan R, Siva A. Synthesis, characterization and aggregation induced emission properties of anthracene based conjugated molecules. *New Journal of Chemistry*. 2016; 40 (6): 5099-5106. doi:10.1039/c5nj03491d

17. Ballesteros LM, Martin S, Pera G, Schauer PA, Kay NJ, Lopez MC, Low PJ, Nichols RJ, Cea P. Directionally Oriented LB Films of an OPE Derivative: Assembly, Characterization, and Electrical Properties. *Langmuir*. 2011; 27 (7): 3600-3610. doi: 10.1021/la104734j

18. Porter MD, Bright TB, Allara DL, Chidsey CED. Spontaneously Organized Molecular Assemblies. 4. Structural Characterization of normal-Alkyl Thiol Monolayers on Gold by Optical Ellipsometry, Infrared-Spectroscopy, and Electrochemistry. *Journal of the American Chemical Society*. 1987; 109 (12): 3559-3568. doi:10.1021/ja00246a011

19. Tsai WY, Taberna PL, Simon P. Electrochemical quartz crystal microbalance (EQCM) study of ion dynamics in nanoporous carbons. *Journal of the American Chemical Society*. 2014; 136 (24): 8722-8728. doi:10.1021/ja503449w